

The STAR Dilepton Physics Program

Frank Geurts (for the STAR Collaboration)¹

Rice University, Houston, TX 77005, USA

Abstract

Dileptons provide ideal penetrating probes of the evolution of strongly-interacting matter. With the Time-of-Flight upgrade, STAR is in a unique position to provide large-acceptance dielectron measurements. We discuss preliminary dielectron results for Au+Au collisions at $\sqrt{s_{NN}} = 19.6 - 200$ GeV, and compare to recent model calculations. With upcoming detector upgrades STAR will further improve its dielectron measurements as well as include dimuon measurements.

1. Introduction

Experimental results from heavy-ion collisions have long established the creation of a new state of hot, dense, and strongly interacting matter [1]. Throughout the evolution of such a system, lepton pairs arise from virtual photons, $\gamma^* \rightarrow l^+l^-$, with its sources varying as a function of the kinematics. Leptons have a very low cross section with the strongly interacting medium. Thus, with negligible final state interactions dileptons provide an excellent penetrating probe of the evolution of a heavy-ion collision. A typical dilepton invariant mass spectrum involves a plethora of sources, ranging from Dalitz decays in the low invariant mass range to Drell-Yan pair production out at higher invariant masses. In between, and in addition to these, we find lepton pairs from vector meson and open heavy-flavor decays, as well as the possible opportunity to detect thermal radiation emitted from a quark-gluon plasma.

The dilepton invariant mass spectra allow us to make divisions that give us an almost chronological view on the evolution of a system. The prominent sources of dileptons in the low mass range (LMR; $M_{ll} < 1.1$ GeV/ c^2), in addition to the Dalitz decays, are the direct decays of the $\rho(770)$, $\omega(782)$, and $\phi(1020)$ vector mesons, generated after the chemical freezeout. The spectral line shape of these mesons may reveal imprints of in-medium modifications possibly related to chiral symmetry restoration. Here, the ρ meson is of special interest given that in thermal equilibrium its yield dominates that of the ω and ϕ mesons [2], and given its relatively short lifetime which is less than the expected lifetime of the system. In the intermediate mass range (IMR; $1.1 < M_{ll} < 3$ GeV/ c^2), the production of dileptons is closely related to the thermal radiation of the Quark-Gluon Plasma (QGP). At higher center-of-mass energies, however, this signal competes with significant contributions from open heavy-flavor decays such as $c\bar{c} \rightarrow e^+e^-X$, where such charm contributions may get modified by the medium, too. Heavy-flavor decays continue to contribute into the high invariant mass region (HMR; $M_{ll} > 3$ GeV/ c^2) in addition to the primordial

¹A list of members of the STAR Collaboration and acknowledgments can be found at the end of this issue.

dileptons from initial hard scattering between the partons of the colliding nuclei, as described by the Drell-Yan processes. Dileptons from the decay of the heavy quarkonia such as the J/ψ and Υ mesons provide means to study deconfinement effects in the hot and dense medium.

Elliptic flow measurements are used to characterize the azimuthal asymmetry of momentum distributions. Dilepton elliptic flow measurements as a function of p_T have been proposed as an independent measure to study the medium properties [3]. The combination of certain transverse momentum and invariant mass ranges allows for different observational windows on specific stages of the expansion. Thus, dileptons can be used to further probe the early stages after a collision and possibly constrain the QGP equation of state.

In 2010, the STAR experiment at RHIC completed its installation of the Time-of-Flight (TOF) detector [4]. The TOF detector brings large-acceptance and high-efficiency particle identification that not only extends the hadron identification reach to higher momenta, but also significantly improves the electron identification in the low momentum range. This, combined with the RHIC Beam Energy Scan program in 2010 and 2011, puts STAR in a unique position to measure dielectron spectra in the low and intermediate mass ranges from top RHIC down to SPS center-of-mass energies. In these proceedings we present new STAR results from dielectron measurements at the RHIC top energy of 200 GeV, as well as first results from measurements at several lower RHIC beam energies. The STAR LMR measurements are compared with recent model calculations. We conclude these proceedings with an outlook on the future STAR dilepton program.

2. Electron Identification and Background Reconstruction

The electron identification for the results reported in the next sections involves the STAR Time Projection Chamber (TPC) and the TOF detector. The TPC detector is the central tracking device of the STAR experiment and provides reconstructed particle tracks and momenta. The energy-loss measurements, dE/dx , in the TPC are used for particle identification. The TOF detector, with full azimuthal coverage at mid-rapidity, extends the particle identification range to higher momenta. The combination of the TOF velocity information and the TPC energy loss allows for the removal of slower hadrons which contaminate the electron sample. With a beam-energy specific selection window and a single track momentum threshold of $p_T > 0.2$ GeV/ c , the electron purity in the minimum bias Au+Au analysis is 95%.

The unlike-sign invariant mass distributions, which are reconstructed by combining electrons and positrons from the same event, contain both signal and background contributions. Especially in high-multiplicity events, the contribution of the combinatorial background is substantial, see Fig. 1. The analyses that are presented in these proceedings use two different methods to determine the background.

The mixed-event method combines electrons and positrons from different events. The events are categorized according to the total particle multiplicity, the event vertex location along the beam axis, and the event plane angle. While the statistical accuracy of the background description can arbitrarily be improved by involving more events, the mixed-event method fails to reconstruct correlated background sources. At the lower invariant masses, such correlated pairs arise from jets, double Dalitz decays, Dalitz decays followed by a conversion of the decay photon, or two-photon decays followed by the conversion of both photons [5]. A background determination in which like-sign pairs of the same event are combined is able to account for such correlated contributions. Its drawback, however, is that the statistical accuracy is only comparable to the

unlike-sign, *i.e.* the original raw mass spectrum. Moreover, the like-sign method will need to consider detector acceptance differences, in contrast to the (unlike-sign) mixed-event method.

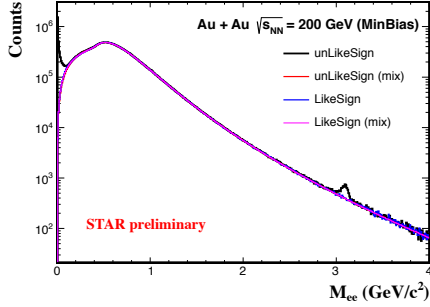


Figure 1: (Color online) Unlike-sign, like-sign, and mixed-event distributions in Au+Au minimum bias collisions at $\sqrt{s_{NN}} = 200$ GeV.

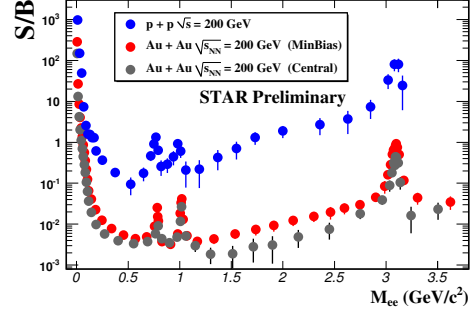


Figure 2: (Color online) Signal-to-background ratios in p+p, and Au+Au central, minimum bias events at $\sqrt{s_{NN}} = 200$ GeV [8].

The like-sign method is applied in the in Au+Au LMR for $M_{ee} < 750$ MeV/ c^2 at $\sqrt{s_{NN}} = 200$ GeV, for $M_{ee} < 900$ MeV/ c^2 for 39 GeV and 62.4 GeV, and throughout the full mass range in 19 GeV [7, 8]. The signal-to-background ratio is shown in Fig. 2.

3. Dielectron Measurements at $\sqrt{s_{NN}}=200$ GeV

STAR recently published the results on its dielectron measurements in p+p at $\sqrt{s} = 200$ GeV [6]. These results were based on 107 million p+p events taken in 2009, with only a partially commissioned TOF system. The agreement between the measured yields and the expected yields from a range of hadronic decays, heavy-flavor decays, and Drell-Yan production, provided an important test of the analysis methods.

Previously at this conference, STAR presented preliminary results of the LMR and IMR invariant mass spectra in both central and minimum bias Au+Au collisions at $\sqrt{s_{NN}}=200$ GeV [8]. In the left panel of Fig. 3, we now present for the same system the centrality dependence of the invariant mass spectra in the STAR acceptance ($|y_{el}| < 1.0$, $|\eta_e| < 1$, and $p_T > 0.2$ GeV/ c). The measured yields are compared to a cocktail simulation of expected yields where the hadronic decays include the leptonic decay channels of the ω , ϕ , and J/ψ vector mesons, as well as the Dalitz decays of the π^0 , η , η' mesons. The input distributions to the simulations are based on Tsallis Blast-Wave function fits to the invariant yields of the measured mesons [5]. These functions are used as the input distributions for the GEANT detector simulation using the full STAR geometry. The ρ meson contributions have not been included in the cocktails as it may be sensitive to in-medium modifications which are expected to affect its spectral line shapes [10]. In the IMR, the $c\bar{c}$ cross section is based on PYTHIA simulations scaled by the number of nucleon-nucleon collisions [9].

In the right panels of Fig. 3, the ratios of the data to cocktail yields have been depicted for different centrality selections. With respect to the cocktail reference a clear LMR enhancement can be observed for each centrality selection. With the cocktail as a reference, only little centrality dependence can be observed. On the other hand, as can be seen in Fig. 4, a comparison of the

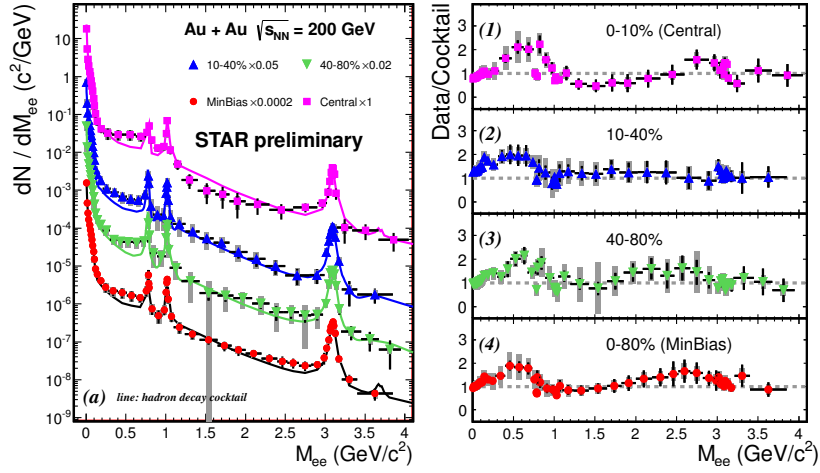


Figure 3: (Color online) Dielectron invariant mass spectra for Au+Au collisions at $\sqrt{s_{NN}} = 200$ GeV for different centrality selections (left panel) and the ratio of data to cocktail (right panel). The systematical uncertainties are indicated by boxes.

dilepton yield dN/dM_{ee} in the range of $150 < M_{ee} < 750$ MeV/ c^2 scaled to the number of participants, N_{part} , clearly indicates an increase of the LMR enhancement with increasing centrality. This agrees with a similar observation in [12].

In the IMR we observe the cocktail simulations to overestimate the data in central collisions. This can indicate a modification of the charm contribution. However, the observed discrepancy is still consistent within the experimental uncertainties. Future detector upgrades will allow STAR to further disentangle the potentially modified charm contributions and provide improved measurements of the thermal QGP dilepton radiation.

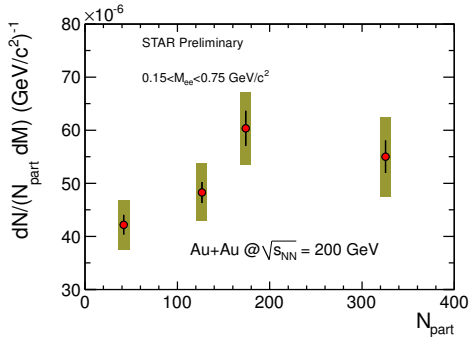


Figure 4: Dielectron LMR enhancement scaled by N_{part} versus centrality (N_{part}) for Au+Au collisions at $\sqrt{s_{NN}} = 200$ GeV [11]. The boxes indicate the systematical uncertainty.

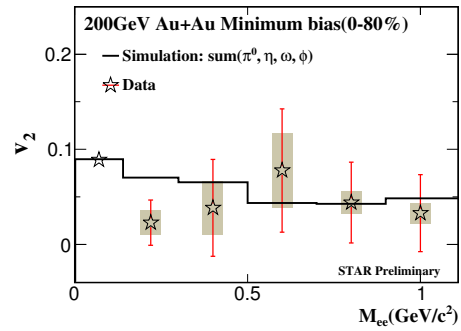


Figure 5: Dielectron elliptic flow as a function of the invariant mass in minimum-bias Au+Au collisions at $\sqrt{s_{NN}} = 200$ GeV. The boxes indicate the systematic uncertainty. The black line is the sum of a simulation which involved π^0 , η , ω , and ϕ -mesons.

In Fig. 5, we present new STAR dielectron elliptic-flow measurements in Au+Au collisions

at $\sqrt{s_{NN}} = 200$ GeV as a function of the dielectron invariant mass. The results are based on 700 million minimum bias events from an analysis that combines data sets from the 2010 and 2011 RHIC runs. The elliptic flow, v_2 , is calculated using the event-plane method in which the event plane has been reconstructed from TPC tracks [13]. The “signal” elliptic flow, v_2^{signal} , is calculated as follows [14]:

$$v_2^{\text{total}}(M_{ee}) = v_2^{\text{signal}}(M_{ee}) \frac{r(M_{ee})}{1 + r(M_{ee})} + v_2^{\text{bkgd}}(M_{ee}) \frac{1}{1 + r(M_{ee})},$$

where v_2^{total} is the flow measurement of all dielectron candidates, v_2^{bkgd} the flow measurement of the dielectron background, and $r(M_{ee})$ the mass-dependent signal-to-background ratio, depicted in Fig. 2. The expected v_2 from a cocktail simulation based on the contributions from π^0 , η , ω , and ϕ mesons is within uncertainties consistent with the measurements.

Differential measurements have been done as a function of centrality (not shown here) and p_T , see Fig. 6. Both $v_2(p_T)$ for different dielectron mass windows, and its centrality dependence in the lower mass bin show a consistency between the measurements and the simulations. Work is underway to further extend these measurements into the IMR. It will be important, however, to disentangle the charm contributions at higher M_{ee} . We observe that the current experimental uncertainties on the STAR data points are still too large to allow for further constraints on the QGP equation of state, as is conjectured in e.g. [3]. However, such a sensitivity is experimentally well within reach with the combination of future data sets, and with an improved understanding of the charm contributions.

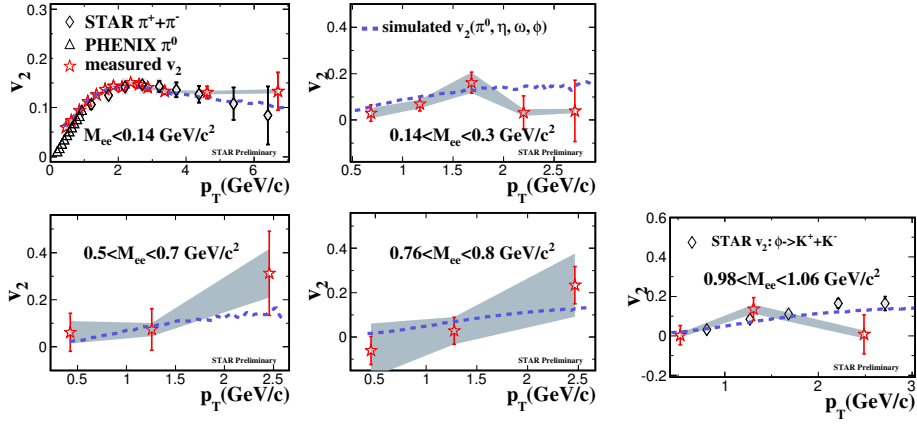


Figure 6: Elliptic flow, v_2 , as a function of p_T for various dielectron invariant mass ranges in Au+Au at $\sqrt{s_{NN}} = 200$ GeV (red stars). In addition, in the upper left panel the v_2 of π^0 [15] and π^\pm mesons [16] are shown. The ϕ meson v_2 measurements in the lower right panel are from STAR. The blue dashed lines are the expected v_2 from cocktail simulations (see text). The grey bands indicate the systematic uncertainties.

4. Dielectron Measurements in the Beam Energy Scan

Measurements performed at top RHIC energies by both STAR and PHENIX [17] have shown a clear LMR enhancement which may point to in-medium modification effects possibly resulting

from chiral symmetry restoration. Measurements performed at the SPS, by the CERES [12, 19] and NA60 [20] collaborations, favor a broadening of the ρ meson spectral function compared to a dropping-mass scenario. With the RHIC BES program, STAR is in a unique position to systematically explore the dilepton production from top RHIC down to SPS center-of-mass energies.

In Fig. 7, the inclusive invariant mass spectra in Au+Au collisions from $\sqrt{s_{NN}} = 19.6$ GeV to 200 GeV are shown, together with the cocktail simulations for each energy. The cocktail simulations exclude contributions from the ρ meson. For each of the energies we observe a significant LMR enhancement. While there remains a quantitative discrepancy between the PHENIX and STAR measurements at $\sqrt{s_{NN}} = 200$ GeV [17, 18], we observe a comparable agreement between the CERES measurements in the Pb+Au at $\sqrt{s_{NN}} = 17.2$ GeV [7, 19].

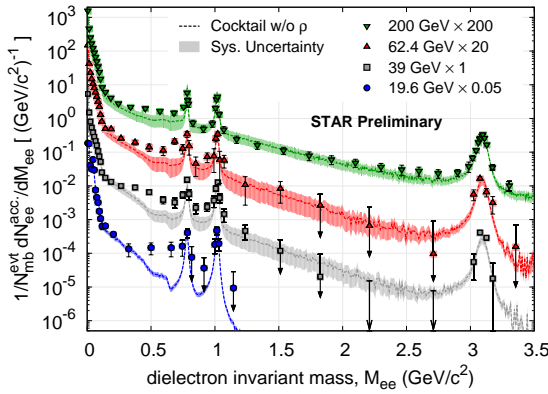


Figure 7: (Color online) Background-subtracted dielectron invariant-mass distributions from Au+Au collisions at $\sqrt{s_{NN}} = 19.6, 39, 62.4,$ and 200 GeV. The (colored) dotted lines show the hadron cocktails (excluding contributions from ρ mesons). The (color) shaded areas indicate the systematic uncertainties.

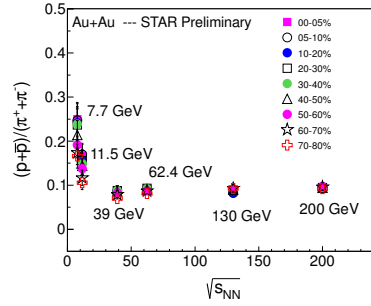


Figure 8: $(p + \bar{p})/(\pi^+ + \pi^-)$ in Au+Au collisions as a function of the center-of-mass energy $\sqrt{s_{NN}}$.

Various models have shown to be in good agreement with LMR spectrum measured by STAR in central Au+Au collisions at 200 GeV [21, 22, 23]. The BES measurements provide an excellent opportunity to further verify robust and consistent model descriptions down to SPS energies. In-medium broadening of the ρ meson is expected to be driven by the strong coupling to baryons and thus the total baryon density since the vector mesons interact symmetrically with baryons and antibaryons [19, 23]. While the net-baryon density will vanish at RHIC top energies, the total baryon density does not change significantly with beam energies down to 20 GeV, as can be seen in Fig. 8.

In Fig. 9, we show the efficiency-corrected invariant mass spectra for minimum bias Au+Au collisions at $\sqrt{s_{NN}} = 19.6, 62.4,$ and 200 GeV, respectively. In each of the three panels the hadron cocktail simulations include contributions from Dalitz decays, photon conversions (19.6 GeV only), and the dielectron decay of the ω and ϕ vector mesons. The cocktail simulations purposely exclude contributions from ρ mesons. Instead, these are explicitly included in the model calculations by Rapp [2, 23] which involve in-medium modifications of the ρ meson spectral shape. In this model a complete evolution of the QGP and thermal dilepton rates in the QGP and hadron-gas (HG) phases are convoluted with an isentropic fireball evolution. In the HG phase the ρ “melts” when extrapolated close the conjectured phase transition boundary. Moreover, it is noted that the top-down extrapolated QGP rates closely coincide with the bottom-up extrapolated

hadronic rates [2].

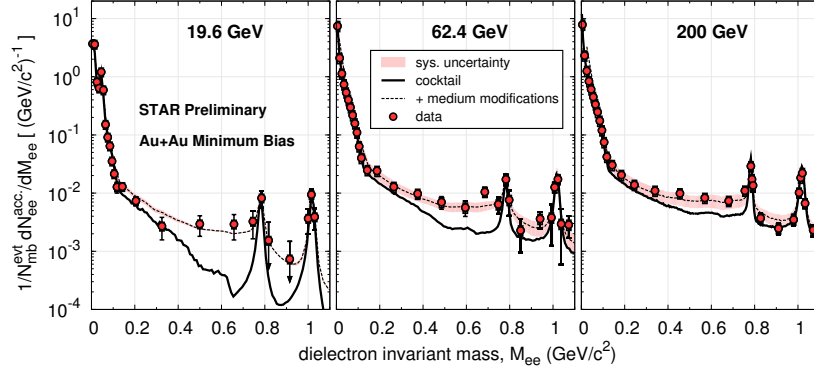


Figure 9: BES dielectron invariant-mass distributions in the low invariant-mass range from Au+Au collisions at 19.6 GeV (left), 62.4 GeV (middle), and 200 GeV (right panel). The red data points include both statistical and systematic uncertainties (boxes). The black curve depicts the hadron cocktail, while the dashed line shows the sum of the cocktail and model calculations. The latter includes contributions from both the HG and the QGP phases. The systematic uncertainty on the former is shown by the light red band.

The LMR enhancement measured by STAR can consistently be described by these model calculations and agrees with a scenario in which the in-medium modification of the ρ involves a broadening of its spectral function. Differential studies of the LMR dielectron distributions as a function of $\sqrt{s_{NN}}$, centrality, and p_T will allow for a more detailed comparison against these chiral hadronic models. Further comparisons between these models, lattice QCD calculations, and experimental data could help provide explicit evidence of chiral symmetry restoration in heavy-ion collisions.

5. Summary and Outlook

Measuring dilepton spectra is a challenging task, where very small signals typically sit on top of large backgrounds. With the recent TOF upgrade, STAR has been able to address some of the important physics questions regarding the LMR enhancement. It has allowed for cross checks with previous measurements on both ends of the BES energy spectrum, as well as systematic, large-acceptance measurements at various other center-of-mass energies. The measurements confirm observations made at SPS energies in which the LMR enhancement is attributed to the broadening of the ρ meson. The model calculations give a robust and consistent picture, and future differential measurements of the BES LMR data will provide an excellent tool to further advance the study of chiral symmetry restoration.

The first years of dielectron measurements at STAR have provided value input to the field, while a number of open questions still remain. As the typical production rates for dileptons are rather small, large event samples are needed to make significantly accurate measurements at increasingly higher invariant masses. Especially at the lower RHIC beam energies, the statistical uncertainties are very large (see Fig. 7). The 19.6 GeV measurements have been based on 28 million Au+Au collisions. To achieve statistical uncertainties at a level of 10% and improve our understanding of the baryonic component to the in-medium effects on the vector mesons, a factor of 10 more statistics would be required. In order to achieve such an increase of an order

of a magnitude in total luminosity, RHIC will need the development and installation of electron cooling components. At top RHIC energy, first results of the LMR dielectron elliptic flow have been presented. These results are found to be consistent with expectations from simulations and other elliptic flow measurements. With an approximate doubling of the currently used combined data sample and an improved understanding of the IMR charm contributions, STAR should be able to distinguish between the HG and QGP v_2 contributions, and help constrain the latter.

Cocktail simulations indicate that the correlated charm contributions dominate the IMR dielectron spectra. The PYTHIA simulations that went into the cocktail simulations assume no medium effects and have been rescaled to match the charm cross sections to, *e.g.*, 0.96 mb in 200 GeV Au+Au collisions. Both assumptions result in large uncertainties, while some hints point to a suppression of the charm contribution in central collisions when compared to the minimum-bias data (see Fig. 3). These uncertainties directly affect the extraction of any IMR dilepton signals related to the thermal QGP radiation. A next round of detector upgrades [24] will further position STAR to significantly improve its measurements of the charm contribution at intermediate dilepton masses. The Muon Telescope Detector (MTD) will enable the measurement of electron-muon correlations, where both leptons are measured at mid-rapidity. The dominant source of IMR $e-\mu$ correlations is $c\bar{c}$ decay, whereas thermal dilepton decay will result in l^+l^- pairs only. Consequently, measuring $e-\mu$ correlations will be an essential tool for isolating the IMR thermal contribution.

The primary focus of the MTD physics program [25] will be on the quarkonia measurements at RHIC energies. However, this large-acceptance muon detector will also allow the STAR dilepton physics program to encompass dimuon spectra and provide for measurements of QGP thermal radiation, light vector mesons, and Drell-Yan production. The MTD is expected to be fully commissioned in 2014.

References

References

- [1] BRAHMS, Nucl. Phys. A 757 (2005), 1; PHOBOS, *ibid.*, 28; STAR, *ibid.*, 102; PHENIX, *ibid.*, 184.
- [2] R. Rapp, J. Wambach, H. van Hees, arXiv:0901.3289v1 [hep-ph].
- [3] R. Chatterjee *et al.*, Phys. Rev. C 75 (2007), 054909.
- [4] W. Llope (for the STAR Collaboration), Nucl. Instr. and Meth. A 661 (2012), S110.
- [5] L. Ruan (for the STAR Collaboration), Nucl. Phys. A 855 (2011), 269.
- [6] L. Adamczyk *et al.*, Phys. Rev. C 86 (2012) 024906.
- [7] B. Huang, these proceedings.
- [8] J. Zhao (for the STAR Collaboration), J. Phys. G: Nucl. Part. Phys. 38 (2011), 124134.
- [9] J. Adams *et al.*, Phys. Rev. Lett. 94 (2005), 062301.
- [10] J. Adams *et al.*, Phys. Rev. Lett. 92 (2004), 092301.
- [11] L. Ruan, *Rapporteur Talk: Heavy Flavor, Quarkonia and Electroweak Probes*, QuarkMatter 2012.
- [12] G. Agakichiev *et al.*, Eur. Phys. J. C 41 (2005) 475.
- [13] B. Adelev *et al.*, Phys. Rev. C 77 (2008), 054901.
- [14] B. Huang (for the STAR Collaboration), Acta Phys. Pol. B Proc. 5 (2012), 471.
- [15] S. Afanasiev *et al.*, Phys. Rev. C 80 (2009), 054907.
- [16] Y. Bai, Ph.D. Thesis, Universiteit Utrecht, The Netherlands (2007).
- [17] A. Adare *et al.*, Phys. Rev. C 81 (2010) 034911.
- [18] F. Geurts (for the STAR Collaboration), arXiv:1208.3437 [nucl-ex]
- [19] D. Adamová *et al.*, Phys. Lett. B 666 (2008) 425.
- [20] R. Arnaldi *et al.*, Eur. Phys. J. 59 (2009) 607.
- [21] O. Linnyk *et al.*, Phys. Rev. C 85 (2012) 024910.
- [22] H. Xu *et al.*, Phys. Rev. C 85 (2012) 024906.
- [23] R. Rapp, Phys. Rev. C 63 (2001) 054907; R. Rapp, private communication.

- [24] H. Huang, these proceedings.
- [25] L. Ruan *et al.*, J. Phys. G: Nucl. Part. Phys. 36 (2009) 095001.